

Available online at [www.sciencedirect.com](http://www.sciencedirect.com)

SCIENCE @ DIRECT®

Journal of Colloid and Interface Science ●●● (●●●●) ●●●●●●

JOURNAL OF  
Colloid and  
Interface Science[www.elsevier.com/locate/jcis](http://www.elsevier.com/locate/jcis)

# AFM study of forces between silica, silicon nitride and polyurethane pads

Igor Sokolov<sup>a,b,\*</sup>, Quy K. Ong<sup>a</sup>, Hasan Shodiev<sup>a</sup>, Nina Chechik<sup>c</sup>, David James<sup>c</sup>, Mike Oliver<sup>c</sup><sup>a</sup> Department of Physics, Clarkson University, Potsdam, NY 13699, USA<sup>b</sup> Department of Chemistry, Center for Advanced Materials Processing, Clarkson University, Potsdam, NY 13699, USA<sup>c</sup> Rohm and Haas Electronic Materials CMP Technologies, Newark, DE, USA

Received 26 December 2005; accepted 7 April 2006

## Abstract

Interaction of silica and silicon nitride with polyurethane surfaces is rather poorly studied despite being of great interest for modern semiconductor industry, e.g., for chemical–mechanical planarization (CMP) processes. Here we show the results from the application of the atomic force microscopy (AFM) technique to study the forces between silica or silicon nitride (AFM tips) and polyurethane surfaces in aqueous solutions of different acidity. The polyurethane surface potentials are derived from the measured AFM data. The obtained potentials are in rather good agreement with measurements of zeta-potentials using the streaming-potentials method. Another important parameter, adhesion, is also measured. While the surface potentials of silica are well known, there are ambiguous results on the potentials of silicon nitride that is naturally oxidized. Deriving the surface potential of the naturally oxidized silicon nitride from our measurements, we show that it is not oxidized to silica despite some earlier published expectations.

© 2006 Published by Elsevier Inc.

**Keywords:** AFM; Surface potential; Surface forces; DLVO; Silica; Silicon nitride; Chemical–mechanical planarization

## 1. Introduction

Interaction of nanoparticles with various surfaces is an interesting topic not only from a fundamental point of view, but also from the applied one. For example, the interaction of silica or silicon nitride with polyurethane surfaces is of great interest for polishing processes used in the modern semiconductor industry. Polyurethane pads are used in the process called chemical–mechanical planarization (CMP) [1–3]. To optimize the CMP process, various chemicals, abrasives, polishing pads, etc. have been investigated [4–12]. However, due to a large number of parameters that can influence the CMP process, the optimization of CMP by experimental means has been difficult. Modeling the CMP process (see, e.g., Refs. [13,14]), can help to rationalize the CMP optimization. To increase the effectiveness of the modeling, one needs to know the behavior of the pad, wafer surfaces, abrasive particles, and their interaction. Silica and silicon nitride wafers and abrasive particles are broadly used in CMP.

The technique that is capable of measuring such information is atomic force microscopy (AFM), see, e.g., [15,16].

From a fundamental point of view, interaction of silica or silicon nitride with polyurethane is interesting because it is virtually unstudied. Furthermore, published reports on studying the surface potentials of silicon nitride, which is naturally oxidized in ambient or aqueous conditions, are somewhat ambiguous. The first work on measuring the force between an oxidized silicon nitride AFM tip and silica surface was done as early as in 1992 by W.A. Ducker and coworkers [17,18], the pioneer in attaching colloidal particles to AFM cantilevers. Lin et al. [19] measured forces between a 30-nm radius SiN AFM tip and a silicon wafer natively oxidized in KNO<sub>3</sub> electrolyte with the concentration of 10<sup>−3</sup> mol/L for a range of acidity, pH 3–11. It was found that the isoelectric point of silicon nitride was close to pH 6. A rather comprehensive study of silicon nitride was done in [20]. That study demonstrated that despite the previous result, the isoelectric point of untreated silicon nitride AFM tip was ca. pH 3 (which is close to silica), while after treatment with hydrofluoric acid for 3 h, it moves to a value between pH 7 and 8.

\* Corresponding author.

E-mail address: [isokolov@clarkson.edu](mailto:isokolov@clarkson.edu) (I. Sokolov).

This work presents the measurements of silicon nitride and silica AFM tips interacting with polyurethane surface of an IC1000™ polishing pad (Rohm and Haas Electronic Materials CMP Technologies). By using a simple linear DVLO approach [21,22], the surface potentials of polyurethane are derived from the measured data of interactions between silica and polyurethane. To test the obtained potentials, we measured the polyurethane zeta potentials independently by the streaming-potentials method [23]. These data are in rather good agreement with the AFM results. Finally, we use the AFM measured interactions between naturally oxidized silicon nitride tip and polyurethane to find the surface potential of the oxidized silicon nitride (here we treat polyurethane potentials derived in the previous step as given). Obtained surface potentials are discussed.

## 2. Materials and methods

### 2.1. Instrumentation

The atomic force microscope used in this study was a Dimension 3100 Nanoscope AFM (DI/Veeco, CA) with built-in video optical system. The AFM operated in contact mode while imaging, and in the force/force-volume modes while measuring the forces. The AFM software v.5.12r4 was employed. Sensitivity of used cantilevers was determined with an assumption that there was no deformation of the tip and sample.

Streaming potential for polyurethane pads was measured by using a commercial Streaming Potential Analyzer with clamping cell (EKA, Brookhaven Instruments, Holtsville, NY) and a reference surface of PMMA. A 10 mM KCl solution was used as a background electrolyte in all the experiments. Potassium hydroxide and hydrochloric acid were used for pH adjustments to study the variation of streaming potential with solution pH. Temperature of the electrolyte solution was maintained at room temperature (22–24 °C) during experimentation.

### 2.2. Materials

Nitric acid of analytical grade (Sigma) and potassium hydroxide (Sigma) were used in this study. Interaction between the tip and pad surfaces was measured in an aqueous solution. Freshly prepared 10 mM KNO<sub>3</sub> background was adjusted with either 10 mM HNO<sub>3</sub> or 10 mM KOH to get the required pH, ranging from 4 to 11. Ultrapure Milli-Q (18 MΩ) water was used for preparing all aqueous solutions. The pH was stable for at least 4–6 h needed to complete a series of the measurements.

### 2.3. Polyurethane pads preparation

A polyurethane pad surface was processed to mimic the actual pad surfaces created during planarization of the CMP process. Specifically, an IC1000™ pad (Rohm and Haas Electronic Materials CMP Technologies) surface was used as received in a CMP tool, WESTECH 372 Polisher. Chemical and topological structure of IC1000 pads was studied before [24].

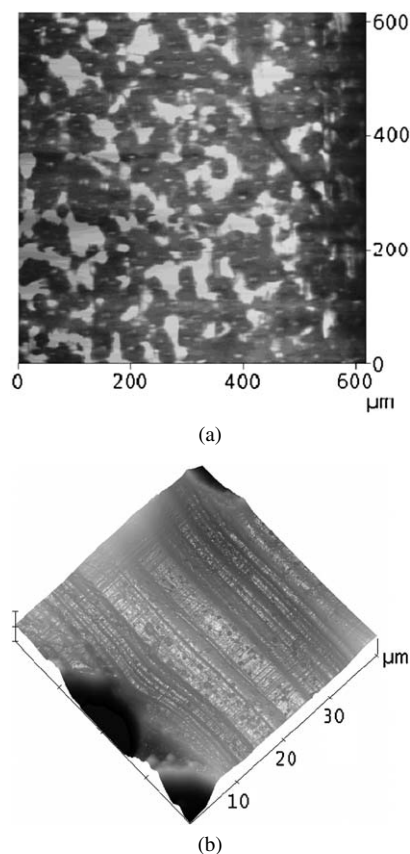


Fig. 1. Processed surface of the polyurethane pad: (a)  $600 \times 600 \mu\text{m}^2$  optical image; (b)  $40 \times 40 \mu\text{m}^2$  AFM image (vertical scale is 1.5  $\mu\text{m}$ ).

Preconditioning was done with SPEEDFAM-IPEC WELDMENT 4" pad conditioner, which contained 68  $\mu\text{m}$  diamond particles. The pad was conditioned by sweeping the diamond grit from the center to the edge of the pad 10 times. The conditioned pad was used for polishing a silicon nitride wafer with Klebosol (silica based) slurry for 25 min at following conditions: carrier speed = 40 rpm, platen speed = 60 rpm, down force = 6 psi, slurry flow = 200 ml/min. Then the slurry was changed to DI water and the polishing of the same wafer was continued for another 20 min. After the polishing, the pad was cleaned with water and ethanol, rinsed with ultrapure water and finally dried by blowing dry air. An example of the surface obtained in this way is shown in Figs. 1a and 1b. Many flat areas are seen in optical image taken by means of the video system of DM3100 Fig. 1a. Fig. 1b shows an  $40 \times 40 \mu\text{m}^2$  AFM image of one of the flat areas of Fig. 1a. It shows sufficient presence of flat regions to do the force measurements.

### 2.4. AFM probes

Standard silicon nitride integrated pyramidal tips (DI/Veeco, Inc.) were used in this study. The spring constant of the cantilevers was  $k \sim 0.17 \text{ N/m}$  (it was found by a resonance method using a built-in option in the AFM software). The radius of curvature of the tips was estimated at  $\sim 40 \text{ nm}$  by scanning of the inverse grid (TGT01, NT-NDT, Inc., Russia), which produced an inverted image of the AFM tip. To remove possible

contaminations of the tip material, the tip was treated with a short-wavelength UV light for 2 min before each experiment. Then the tip (cantilever) was immersed into  $10^{-2}$  M  $\text{KNO}_3$  background solution for 2 h to induce “aging” of the tip surface.

Silica covered tip was obtained as follows. A standard RSET silicon tip with initial nominal tip radius  $<10$  nm was oxidized in air during 2 h in  $1000^\circ\text{C}$  as described in [25]. The tip was immersed in aqueous solution of pH 9 to age the obtained silica surface (to recover enough silanol groups). The radius of curvature was found to be ca. 250 nm by the mentioned above scanning of the inversed grid.

### 2.5. Force measurements

Standard force-volume mode of AFM operation was used. Using this mode was justified by its ability to visualize the surface topography while collecting the force curves at each point. To test a possible AFM tip contamination, we measured force curves between each tip and a freshly polished silica wafer before and after each series of tests. The clean tips were expected to show the same force curves before and after each series of tests. Approach force curves were used for the force analysis (Figs. 2 and 5), while the retracting curves were processed to obtain adhesion data (Figs. 4 and 8).

## 3. Results and discussion

The silica interaction with the polyurethane pad was measured by averaging of ca. 10 the most representative force curves for each pH. The results are shown in Fig. 2. The observed dependence can be analyzed in the frame of a theoretical approach (known as the DLVO theory) for modeling the force between the AFM tip and a surface as a function of the tip-surface distance, the pH and ionic strength of the solution, and the geometry of the tip and the surface. Specifically, we con-

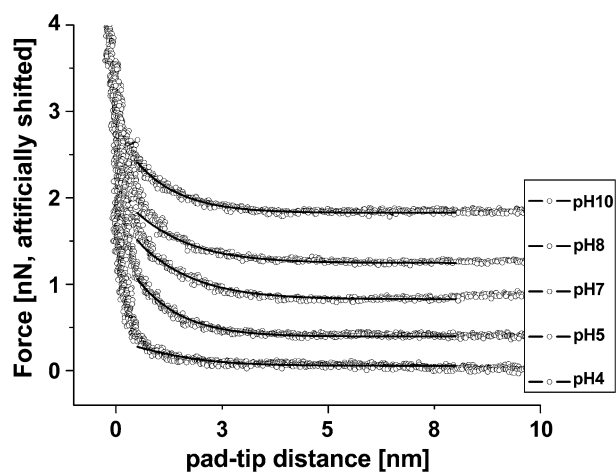


Fig. 2. Forces acting between silica tip and polyurethane pad for various acidities. Each force curve is artificially shifted in a vertical direction for better visualization. Solid lines correspond to the theoretical fitting curves. Distances less than 0.5 nm were not taken into account while fitting.

sider the tip-surface force  $F$  the following sum

$$F = F_{\text{EDL}} + F_{\text{vdW}}, \quad (1)$$

where  $F_{\text{vdW}}$  is the London-van der Waals force, and  $F_{\text{EDL}}$  is the electrical double layer force. In fact, this is a sufficiently powerful and accurate approach for describing a variety of phenomena in colloid science, even though other possible forces such as hydration, solvation, steric, etc. forces are neglected in this description.

Results for the London-van der Waals force, which is usually attractive in nature, are given for a variety of geometries in [22,26,27]. In the first-order approximation, all those approaches provided the same result for either spherical or parabolic asperity of the AFM tip (or for a spherical particle of the same radius  $R$ ),  $F_{\text{vdW}} = AR/6d^2$ , where  $A$  is the Hamaker constant,  $d$  is the distance between the AFM tip and the surface of interest.

Results for the electrostatic force can be obtained by solving the Poisson-Boltzmann equation for the potential distribution in the liquid, subject to suitable boundary conditions. These conditions are usually either of the form of a prescribed constant surface potential or a prescribed constant surface charge density on each boundary. The Poisson-Boltzmann can be solved either in a linear or non-linear approximations. The linear approximation employs the simple well-known solution of the linearized Poisson-Boltzmann equation for the electrostatic interactions between two flat plates separated by a fluid [28]. The non-linear approximation employs the solution of the fully non-linear Poisson-Boltzmann equation. This solution was originally obtained and reported in [29]. A more detailed investigation of the solution is presented in [30]. A numerical solution of the non-linear Poisson-Boltzmann equation for the interaction between two spheres and the interaction between a sphere and a flat plate was obtained in [31], and evaluated the utility of the non-linear Derjaguin approximation, as well as that of the linear Derjaguin approximation. In addition, those authors compared the numerical solution of the linearized Poisson-Boltzmann equation with the numerical solution of the non-linear Poisson-Boltzmann equation as well as so-called weak overlap approximation. As one can see for those analyses, the linear approximation and the weak overlap approximation are relatively good ones. Taking into account those results, and comparing them with the error-bar of our measurements (which is relatively large, see below), we choose to use these approximation to calculate  $F_{\text{EDL}}$ . Following [28], one has for the case of linear approximation

$$F_{\text{EDL}}(d) = 4\pi\epsilon\epsilon_0\kappa\psi_1\psi_2R\exp(-\kappa d), \quad (2)$$

where  $\epsilon_0$  is the permittivity of free space,  $\epsilon$  the permittivity of medium,  $\psi_1$  and  $\psi_2$  are the surface potentials of the sphere and the surface, respectively,  $\kappa^{-1}$  is the Debye length, which is a measure of the thickness of the electrical double layer

$$\kappa = \sqrt{\frac{e^2 \sum_i z_i^2 n_i}{\epsilon\epsilon_0 k_B T}}. \quad (3)$$

Here  $z_i$  are the ion valences,  $n_i$  are the ion concentrations, and  $T$  is the temperature of the electrolyte. However, formula (2)

works good while the surface potentials are less than  $\sim 30$  mV. For the surface potentials less than  $\sim 100$  mV (while  $d \gg 1/\kappa$ ) one can use the weak overlap approximation. EDL force in that approximation is given by

$$F_{\text{EDL}} = (128\pi RkT\rho_{\infty}/\kappa) \tanh\left[\frac{ze\psi_1}{4kT}\right] \tanh\left[\frac{ze\psi_2}{4kT}\right] \times \exp(-\kappa d), \quad (4)$$

where  $k$  is the Boltzmann constant,  $\rho_{\infty}$  is concentration of counterions far from the surfaces. To find the surface potential, we will first use Eq. (2). However, if the obtained potential is greater than 30 mV, we will use Eq. (4). In this work we will not deal with the surface potentials greater than 100 mV.

Finally, since it is very hard to measure the absolute zero tip–surface distance in the AFM measurements, we introduced an offset  $d_0$ , which is treated as a free parameter. Typically the values of  $d_0$  depend on nanoroughness and nanodeformations. Non-zero  $d_0$  occurs also from impossibility to reach distances of direct contact interactions ( $\sim 0.5$  nm). In our fittings this value range was kept within  $\pm 1$  nm. Furthermore, we assumed that the unknown Hamaker constant for polyurethane–water–glass or polyurethane–water–silicon nitride in aqueous solution was in the range of  $10^{-20}$ – $10^{-21}$  J. It is plausible to assume due to known low variability of the Hamaker constant. Variation of this constant is included in the “error bar.” After all, the fitting of experimental data was done with the following formula

$$F = -\frac{AR}{6(d+d_0)^2} + F_{\text{EDL}}, \quad (5)$$

where the potential  $\psi$  is expressed in volts,  $M$  is the buffer molarity, both  $R$  and  $d$  are in meters.  $F_{\text{EDL}}$  can conveniently be rewritten for the linear approximation as

$$F_{\text{EDL}} = 28.91\sqrt{M}\psi_1\psi_2R \exp\left(-\sqrt{M}\frac{d+d_0}{0.302 \times 10^{-9} \text{ m}}\right), \quad (6)$$

or the weak overlap approximation as

$$F_{\text{EDL}} = 0.303R\sqrt{M} \tanh\left[\frac{\psi_1}{0.103}\right] \tanh\left[\frac{\psi_2}{0.103}\right] \times \exp\left(-\sqrt{M}\frac{d+d_0}{0.302 \times 10^{-9} \text{ m}}\right). \quad (7)$$

It should be noted that the molarity of the buffer in which we did the force measurements was increased with time for the silica–polyurethane force measurements due to water evaporation. This occurred due to the instrumental issue of the used AFM, the fluid cell of Nanoscope DM3100 is open. A relatively long time for test measurements was needed due to the fact that the oxidized to silica AFM tip was on a rather rigid cantilever. To do scanning with such a tip, we had to use the tapping mode, which was rather slow comparing to the contact mode, which we used with the silicon nitride tip. For the time of scanning some water can evaporate and, consequently, slightly change the ionic strength of our solution.

Fitting curves are shown directly in Fig. 2. One can see a fairly good agreement with Eq. (5). However, there is a considerable deviation for the distances less than 0.5 nm. This

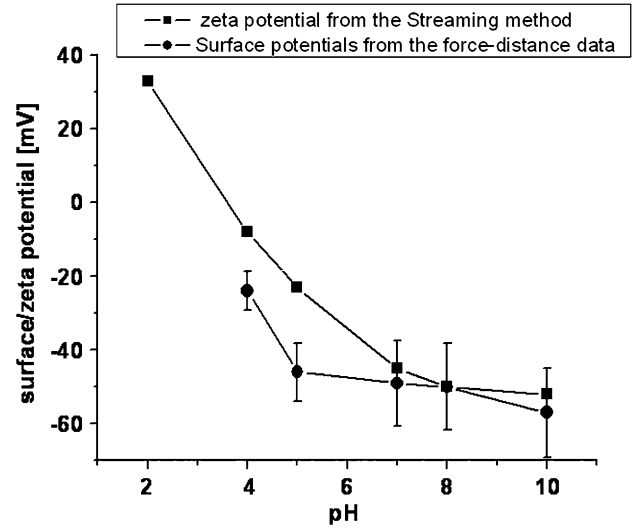


Fig. 3. Surface potentials of polyurethane derived from the force measurements in comparison with zeta potentials estimated in the method of streaming potential.

can presumably be explained by the existence of nanoroughness. Therefore we did not take into account distances less than 0.5 nm while fitting these force curves. Fig. 3 shows the results of fitting the force curves of Fig. 2 with formula (5). The error bar was found in the non-linear fit procedure by using Origin software. It should be noted that silica surface potential was taken as a known parameter, see, e.g., Ref. [32]. These potentials are plotted later in Fig. 6 for comparison with the fitted silicon nitride potentials. To check if the fitted polyurethane potentials are reasonable, measurements of zeta potentials of polyurethane surfaces were done with the streaming potentials method. Fig. 3 also shows these zeta-potentials. Comparing these potentials, one can see that the fitted surface potentials have rather reasonable values. Some difference can be explained by the fact that the AFM tip probes the potential much deeper into the layer of compensating ions. In addition, the streaming potential method is still not well developed for surface with non-planar geometry like our pad. The results of measurements of adhesion between the silica tip and the pad are shown in Fig. 4. Each point is an average of ca. 100 measurements over  $1 \mu\text{m}^2$  area, the variation-bar corresponds to one standard deviation.

The force measurements of silicon nitride tips are shown in Fig. 5. These measurements were done in the same manner as above. The only difference was that the averaging was done over ca. 1000 force curves. This is explained by the fact that the radius of the silicon nitride tips is about five times smaller than the radius of the silica tip used before. Due to larger area of contact, each measurement with a duller tip was effectively equivalent to an average of multiple measurements with sharper tips. Therefore, to get comparable statistics one should do more measurements with sharper tips. However, the noise was averaged out better in Fig. 5 than in Fig. 2.

Fitting of the EDL potentials was done in the same way as in the above case of silica–polyurethane interaction. However, in the present case we have to take into consideration the surface

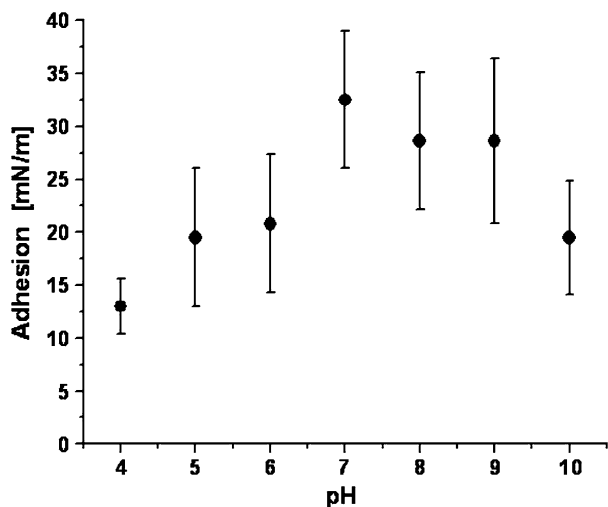


Fig. 4. Adhesion between the silica tip and the pad. The adhesion forces normalized on the tip radius are shown.

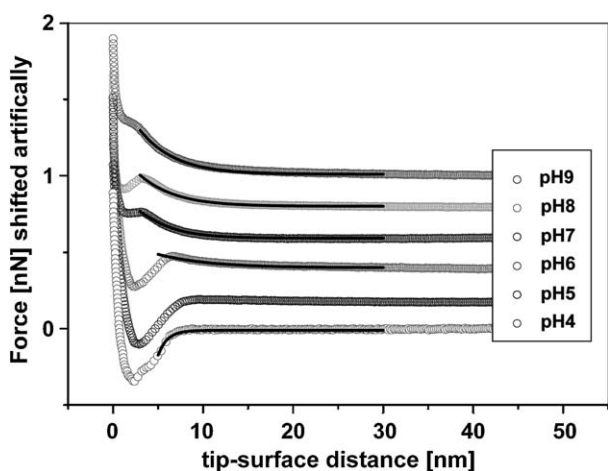


Fig. 5. Forces acting between silicon nitride tip and polyurethane pad for various acidities. Each force curve is artificially shifted in a vertical direction for better visualization. Solid lines correspond to the theoretical fitting curves. Distances less than 5 nm were not taken into account while fitting.

potentials of silicon nitride and polyurethane. Because the potentials of polyurethane were obtained above, Fig. 3, we used them as a given. At the same time, the surface potentials of silicon nitride were derived from the force–distance data.

There was another specific feature of the force curves shown in Fig. 5. As the AFM tip approached the surface, it experienced some repulsion for the cases of pH greater than 5. After the tip passed some threshold, however, the force curves broke down. This happened due to the known disbalance of gradient of attraction forces and the spring constant of the cantilever (see, e.g., [16]). For example, if the major contributor of the attraction is the van der Waals force, close to the surface the gradient of the van der Waals force keeps increasing while the cantilever spring constant stays the same. When the attraction gradient exceeds the spring constant the cantilever becomes unstable and “jumps” to the surface. The breaks in the force curves were not seen in Fig. 2 because of much higher spring constants of the AFM cantilevers that were used there.

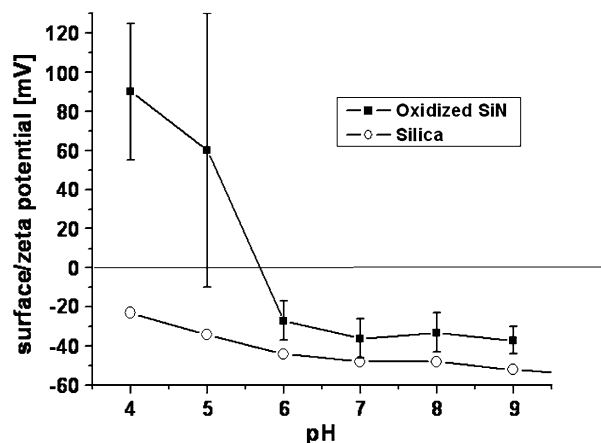


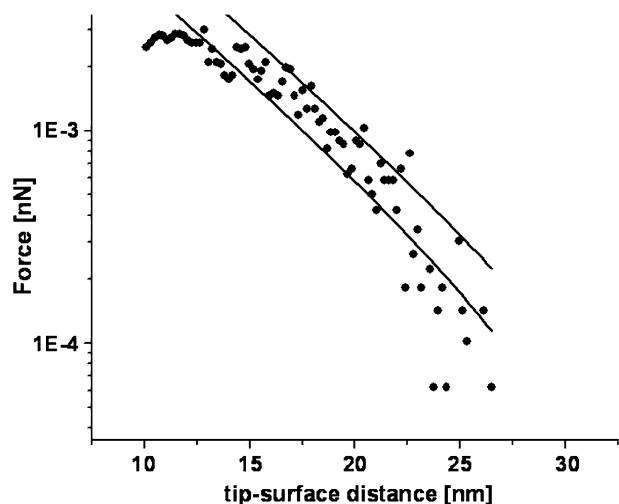
Fig. 6. Surface potentials of naturally oxidized SiN derived from the force measurements. Surface potentials for silica are shown for comparison.

To find the surface potentials, we use the force curves for distances greater than positions of those breaks (distances greater than  $\sim 5$  nm). This was simple and unambiguous for cases of pH 6 and higher when we deal with repulsion. The results are presented in Fig. 6. The cases of pH 4 and 5 required special explanation because of strong attraction force. Let us consider first the force curve of pH 5.

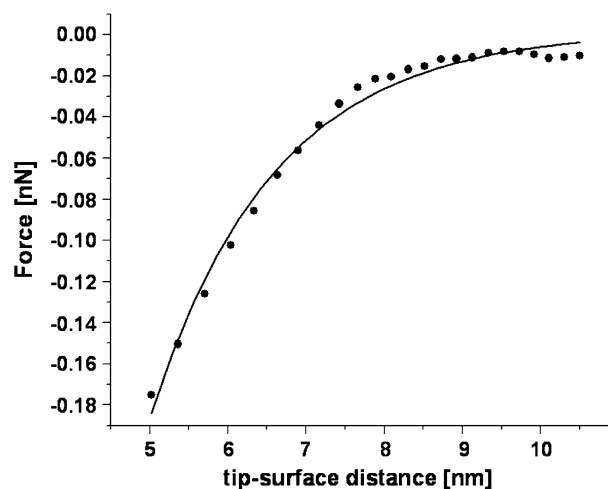
Actually, there was also some initial repulsion here. However, it was rather small. Fig. 7a shows a part of the force curve in logarithmic scale for the distance interval between 10 and 30 nm. Fig. 6a also demonstrates two different fitting curves. The upper curve corresponds to the surface potential of silicon nitride of  $-20$  mV, while the lower curve is drawn for  $-10$  mV. This variation is a typical for all our fittings. The problem, however, is that this force is very small. It can be seen only due to the averaging of the force curves. For a single force curve, the noise is an order of magnitude higher than this force value. Consequently, this result is not completely reliable. Considering smaller distances, one can see attraction. Fig. 7b. shows the region of initial attraction, when the tip starts to deflect down. Interestingly, this behavior cannot be explained by the van der Waals attractive forces, which are too small for such large distances. Following our model, we have to assume that we are dealing with the EDL attraction. The solid line in Fig. 7b shows a fit with the EDL attraction that corresponds to the silica nitride surface potential of ca.  $+70$  mV. To show this ambiguity in definition of the surface potential, we put additional possible negative potential on the graph of Fig. 7.

The case of pH 4 was similar to the attractive case of pH 5 shown in Fig. 7b. However, there was no repulsive part as in the case of pH 5. Limited number of points recorded in that region still resulted in a relatively large error-bar in definition of the surface potential shown in Fig. 6.

To compare these potentials with silica ones, we plot the silica potentials on the same graph. One can clearly see the difference. To amplify the difference between the oxidized silicon nitride and silica tips, adhesion between the silicon nitride and polyurethane was measured in the same manner as in the case of



(a)

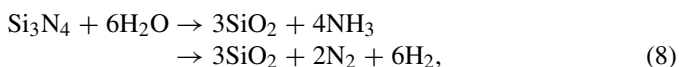


(b)

Fig. 7. Zoomed force curves for the case of pH 5 of Fig. 6. Solid lines show the theoretical fittings.

silica–polyurethane shown in Fig. 4. The results are presented in Fig. 8. One can see quite an opposite dependence on pH.

Let us address the difference between oxidized silicon nitride and silica in more detail. A rather classical point of view was presented in [33], where it was suggested that oxidation of silicon nitride towards silica takes only minutes via the following reactions:



see also [34–36]. It is known that the isoelectric point of silica is between 2 and 3. As one can see from Fig. 6, the isoelectric point of naturally oxidized silicon nitride tip lies at least between 4 and 6 (seen as the absence of long-range repulsion). Therefore, this demonstrates that silicon nitride oxidized in a natural environment cannot be covered by silica, at least completely. It has to be noted that this result is in agreement with reports in [19,35], while contradicts [20]. The latter can probably be addressed to difference in the tip preparation. Specifically, [20] used 100 W plasma reactor for preliminary tip cleaning. This could have created the expected layer of silicon oxide.

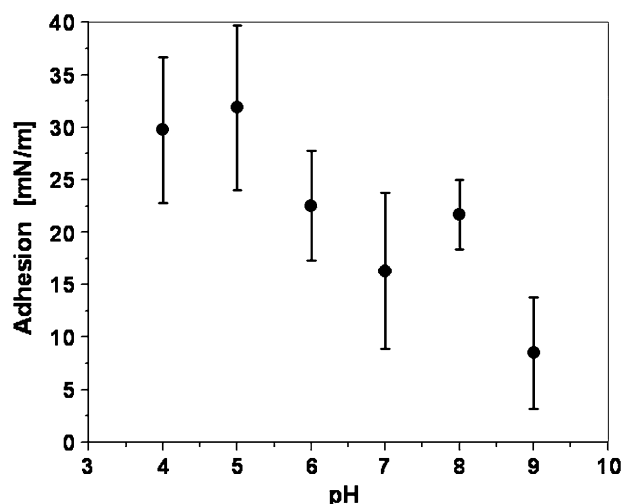


Fig. 8. Adhesion between the SiN tip and pad. The adhesion forces normalized on the tip radius are shown.

#### 4. Summary

The interaction of silica and silicon nitride AFM tips with polyurethane surfaces were measured by AFM in aqueous solutions of different acidity, at pH = 4–10. Surface potentials of polyurethane were derived from the measured data. The obtained potentials were in rather good agreement with measurements of zeta potentials using the streaming-potentials method.

While the surface potentials of silica are well known, there were ambiguous results on the potentials of silicon nitride that was naturally oxidized in buffers. Deriving the surface potential of the naturally oxidized silicon nitride from our measurements, we showed that it was not oxidized to silica despite some expectations in the literature. Another important parameter, adhesion was also measured for silica–polyurethane and silicon nitride–polyurethane. Comparison of the adhesion also demonstrated the difference between the naturally oxidized silicon nitride and silica tips.

#### Acknowledgment

Financial support from Rohm and Haas Electronic Materials CMP Technologies is acknowledged.

#### References

- [1] Solid State Technology, special December issue, 72 (2000).
- [2] S.V. Babu, in: K.C. Cadien, H. Yano (Eds.), Chemical–Mechanical Polishing, MRS Publishing, 2001, p. 671.
- [3] S.V. Babu, S. Danyluk, in: M. Krishnan, M. Tsujimura (Eds.), Chemical–Mechanical Polishing: Fundamentals and Challenges, MRS Publishing, 1999, p. 566.
- [4] Q. Luo, D.R. Campbell, S.V. Babu, Langmuir 12 (1996) 3563.
- [5] M. Hariharaputhiran, J. Zhang, S. Ramarajan, J.J. Keleher, Y. Li, S.V. Babu, J. Electrochem. Soc. 147 (2000) 3820.
- [6] A. Jindal, S. Hegde, S.V. Babu, Electrochem. Solid State Lett. G 48 (2002) 5.
- [7] D. Zeidler, Z. Stavreva, M. Plotner, K. Drescher, Microelectron. Eng. 33 (1997) 259.
- [8] R. Carpio, J. Farkas, R. Jairath, Thin Solid Films 266 (1995) 238.

- [9] Q. Luo, R.A. Mackay, S.V. Babu, *Chem. Mater.* 9 (1997) 2101.
- [10] Y. Li, M. Hariharaputhiran, S.V. Babu, *J. Mater. Res.* 16 (2001) 1066.
- [11] A. Jindal, Y. Li, S.N. Barayanan, S.V. Babu, *Mat. Res. Soc. Symp. Proc.* 671 (2001) M4.10.1.
- [12] Y. Li, S.V. Babu, *Electrochem. Solid State Lett.* 148 (2001) G20.
- [13] G. Ahmadi, X. Xia, *J. Electrochem. Soc.* 148 (2001) G99.
- [14] R.S. Subramanian, L. Zong, *Thin Solid Films* 397 (2001) 143.
- [15] G. Binnig, H. Rohrer, *Helv. Phys. Acta* 55 (1982) 726.
- [16] I. Sokolov, *Appl. Surf. Sci.* 210 (2003) 37.
- [17] W.A. Ducker, T.J. Senden, R.M. Pashley, *Nature* 353 (1991) 239.
- [18] W.A. Ducker, T.J. Senden, R.M. Pashley, *Langmuir* 8 (1992) 1831.
- [19] X.-Y. Lin, F. Creuzet, H. Arribart, *J. Phys. Chem.* 97 (1993) 7272.
- [20] B.V. Zhmud, A. Meurk, L. Bergstrom, *J. Colloid Interface Sci.* 207 (1998) 332.
- [21] J. Israelachvili, *Intermolecular and Surface Forces*, second ed., Elsevier/Academic Press, San Diego, 1992.
- [22] I. Sokolov, *Surf. Sci.* 311 (1994) 287.
- [23] E.M. Vrijenhoek, M. Elimelech, *Langmuir* 18 (2002) 2193.
- [24] H. Lu, B. Fookes, Y. Obeng, S. Machinski, K.A. Richardson, *Mater. Charact.* 49 (2002) 35.
- [25] G. Huttli, D. Beyer, E. Muller, *Surf. Interface Anal.* 25 (1997) 543.
- [26] J. Mahanty, B.W. Ninham, *Dispersion Forces*, Academic Press, London, 1976.
- [27] P.C. Hiemenz, R. Rajagopalan, *Principles of Colloid and Surface Chemistry*, Dekker, New York, 1997.
- [28] H. Ohshima, *J. Colloid Interface Sci.* 198 (1998) 42–52.
- [29] O.F. Devereux, P.L. de Bruyn, *Interaction of Plane Parallel Double Layers*, MIT Press, Cambridge, 1963.
- [30] D. McCormack, S.L. Carnie, D.Y.C. Chan, *J. Colloid Interface Sci.* 169 (1995) 177.
- [31] J. Stankovich, S.L. Carnie, *Langmuir* 12 (1996) 1453.
- [32] A. Feiler, I. Larson, P. Jenkins, P. Attard, *Langmuir* 16 (2000) 10269.
- [33] T.E. Fisher, W.M. Mullins, *J. Phys. Chem.* 96 (1992) 5690.
- [34] R.K. Iler, *The Chemistry of Silica*, Wiley, New York, 1979.
- [35] L. Bergström, E. Bostedt, *Colloids Surf.* 49 (1990) 183.
- [36] L. Bergström, R.J. Pugh, *J. Am. Ceram. Soc.* 72 (1989) 103.